The Influence of Fish on the Mooring Loads of a Floating Net Cage

Zhao He[a,*], Odd Magnus Faltinsen[a,b], Arne Fredheim[c], Trygve Kristiansen[a]

[a] *Department of Marine Technology, Norwegian University of Science and Technology NO-7491, Trondheim, NORWAY*
[b] *Centre for Autonomous Marine Operations and Systems (AMOS), Norwegian University of Science and Technology, NO-7491, Trondheim, NORWAY*
[c] *SINTEF Fisheries and Aquaculture, NO-7465, Trondheim, NORWAY*

Abstract

The influence of fish on the mooring loads of a floating net cage is studied numerically and experimentally. Two experimental series were conducted. One case was model tests with artificial fish. Nine rigid fish models with total volume of 2.5% of the fish cage at rest were placed inside the net cage without touching the net and towed with the net cage. The other case was live fish experiments in waves and current where more than 800 salmons of length 16 cm occupied about 2.5% of the fish cage volume at rest. The flow-displacement effect of a rigid fish in current was simulated by a potential-flow slender-body theory. Viscous wake effects were added. The displacement flow is clearly more important than the viscous wake flow. Both the numerical simulations and the model tests with rigid fish in current show that the fish influence on the mooring loads of the fish cage is less than 3% of the mooring load without fish. However, the measured mooring loads with live fish in current are between 10% and 28% larger than without fish. The reason is contact between the fish and the net cage. Accounting for the latter fact in the numerical model by changing the local solidity ratio of the net in the contact area gave reasonable numerical predictions. The experiments in waves and combined waves and current also showed a non-negligible influence of the fish on the mooring loads. The waves influenced the behaviour of the fish

*Corresponding author
Email address: zhao.he@ntnu.no (Zhao He)

and some of the fish went to the net bottom possibly due to that they were uncomfortable in the wave zone.
Keywords: fish farm, fish influence, mooring loads, model tests, numeric

1. Introduction

Structural failure of the net cage is a main reason for fish escape in Norway (Jensen et al., 2010)[1]. Since an increase in marine fish farming in more exposed areas is expected, fish farm structures will be subjected to more intensive sea conditions. Making a more robust fish farm system requires a detailed study of every aspect of the fish farm.

The fish occupy up to 2.5% of the volume of the net cage at rest. The presence of fish will influence the flow through and inside the net cage and thereby affect the oxygen consumption of the fish as a function of the dissolved oxygen level of incoming water, water exchange and biomass inside each cage. Some researchers focused on the effect of fish behavior on the flow and the water exchange in net cages (Chacon-Tonnes et al., 1988)[2], but none of them studied the hydrodynamic influence on the loads on the net cage.

Laursen et al.(2014)[3] studied the behavior of salmon swimming in a fish farm cage in a current. In their field measurements, they observed that at high current velocities the salmon switched from the traditional circular polarized group structure, seen at low and moderate current velocities, to a group structure where all fish kept stations at fixed positions swimming against the current. Winthereig-Rasmussen et al. (2015)[4] presented full-scale measurements of current dominated velocities in the wake of the aquaculture farm Gulin consisting of ten gravity-type sea cages in a 2×5 grid anchored in the bay of Thorshavn. Rasmussen et al. (2016)[5] compared the latter experiments with Computational Fluid Dynamics (CFD). They suggested that the clear differences between experimental and numerical results were due to the influence of fish. Since error sources such as approximating the net as a porous media and neglecting net deformation in the numerical calculations were not quantified, their studies do

not show how much influence the fish has on the flow. Our experimental studies do not investigate flow details. However, the clear influence shown in the main text that living fish has on the net drag force implies by conservation of fluid momentum that there is a non-negligible influence on the flow velocity.

A CFD method is very time consuming and unrealistic to use in simulating the behavior of all fish present in a fish farm. To what extent approximate methods can be used, is a matter of future research. If we can neglect fish-fish interaction, the single fish models by Newman and Wu (1973)[6] and Wolfgang et al. (1999)[7] can be investigated. Newman and Wu (1973)[6] used a generalized potential-flow slender-body theory and Wolfgang et al. (1999)[7] applied a 3D boundary element method (BEM).

Our objective is to study experimentally and partially numerically the influence of a fish group on the mooring loads in current and waves on a net cage with a circular inelastic floater. Both rigid artificial fish and live fish are used. However, fish behavior is an unknown variable and we do not know if the fish behave similarly in model tests as in full scale.

2. Numerical modelling of rigid fish model in current

In the numerical modelling of rigid artificial fish, axisymmetric fish bodies that do not touch the net is assumed. Hydrodynamic propulsion is neglected. The hydrodynamic influence of the fish on the mooring loads of the net cage is mainly due to the influence on the incident flow to the front and rear part of the net cage. Both the wake flow and the displacement flow of the fish body matter.

In describing the wake flow, we consider an axisymmetric fish body with a hydraulically smooth surface in an infinite fluid and with an incident constant flow velocity U_i in the longitudinal fish direction. In our considered Reynolds numbers, the boundary layer flow is laminar while the wake is turbulent. Assuming the wake is fully developed behind a smooth and streamlined body, the axisymmetric longitudinal mean turbulent wake flow velocity u can be calcu-

lated according to Blevins (1984)[8] by equation (1).

$$\frac{u}{U_i} = 1 - 0.35\left(\frac{C_{Dfish}S_s}{x}\right)^{2/3} exp[-1.9r^2(xC_{Dfish}S_s)^{-2/3}] \tag{1}$$

Here, S_s is the total wetted surface area of one fish, r is the radial distance from the extended centerline of the fish body and x is the axial distance from the origin of the wake at the front end of the fish. C_{Dfish} is the drag coeffiecient of the fish with laminar boundary layer flow, which according to Blevins (1984)[8] can be calculated by $C_{Dplate}[1+(\frac{2B}{L})^{2/3}]+0.11(\frac{2B}{L})^2$, where $C_{Dplate} = \frac{1.328}{\sqrt{U_iL/\nu}}$ is the drag coefficient of a plate with length L. 2B is the width of the fish, and L is the length of the fish.

The fact that the fish displace the water causes a displacement flow. Here, we assume no hydrodynamic interaction between the fish, and an infinite fluid domain with potential flow is considered. We use an inertial coordinate system moving with the forward speed U of the fish, where the origin of the coordinate system is fixed at the front end of the middle fish as shown in Figure 1. For each fish, the total velocity potential is expressed as $\Phi = Ux + \varphi_1$ where the x-axis is parallel with the longitudinal direction of the fish. Positive x is in the aft direction of the fish. Slender-body theory is used and we solve the problem by matched asymptotic expansions between far-field and near-field solutions (Newman, 1977)[9]. In the far field of the fish body, the fish influence can be treated as a source distribution along the body axis. The total flow velocity potential $\Phi(x, y, z)$ in the far-field can be calculated by equation (2).

$$\Phi(x, y, z) = Ux - \frac{1}{4\pi}\int_{x_H}^{x_T} \frac{Q(\xi, t)d\xi}{[(x-\xi)^2 + y^2 + z^2]^{0.5}} \tag{2}$$

Here, $Q(\xi, t)$ is the source density, which follows by matched asymptotic expansions between the far-field and near-field solutions (Newman, 1977)[9], x_H and x_T represent the x coordinates of the fish head and edge of the fish tail, respectively.

Knowing the source density, the flow velocity in the far field can be calculated. Since we neglect hydrodynamic interaction, the contribution from each

fish to the inflow on the net is simply added. The procedure assumes implicitly that the fish are in each others far field and that the net is in the far-field of the fish. According to Skejic and Faltinsen (2008)[10], the far-field assumption gives quite good results even though the transverse distance between two equal (axisymmetric) bodies on parallel course is of the order of the body beam.

How relevant is the hydrodynamic analysis of the artificial fish for a live fish when the fish stays in the far field of the net? A real fish will also cause a displacement flow represented in terms of a source distribution. The transverse motions of a real fish can be represented in the far field by a distribution of transverse dipoles along the fish. Dipoles decay more rapidly than sources in the far field. Furthermore, it follows by conservation of fluid momentum for a self-propelled live fish on a straight course with constant speed that the longitudinal momentum fluxes associated with fish resistance and propulsion must balance. Since it turned out that the displacement flow was dominant, it means that our far-field analysis of the artificial fish gives representative flow velocities for a live fish as long as the displaced volumes are similar and the fish remain stationary and sufficiently far from the net.

The hydroelastic net cage model by Kristiansen and Faltinsen (2012a)[11] is used, which implies that the net deforms due to the hydrodynamic loads and the hydrodynamic loads are affected by the time-varying net position. An equivalent truss model is applied. The mass of trusses of the model are lumped into the nodes connecting the trusses. The tension in the trusses are solved at each time step and the viscous hydrodynamic forces are calculated by using a screen-type empirical model. The node positions are time stepped according to Newtons second law. A screen-type hydrodynamic model implies that both normal and tangential loading on a net panel is considered. It involves pressure loss coefficients, which are functions of the Reynolds number of individual twines and the solidity ratio Sn, which is one minus the open area ratio of the net. The cross-sectional shape of twines is approximated by a circular section and the Reynolds number dependent drag coefficient for smooth circular cylinder is one of the parameters in the model. The formula depends on the inflow

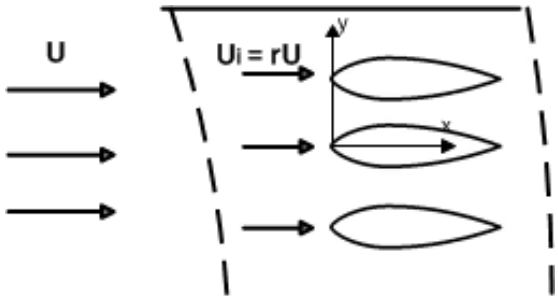

Figure 1: The wake flow after the front net cage: U is the ambient incoming flow velocity, $U_i = rU$ is the incident flow velocity to the fish and r is the reduction factor due to the front net. The fish represents an additional source of flow disturbance. The origin of the coordinate system is fixed at the front end of the middle fish. The size of the fish is exaggerated for illustrative purposes.

direction relative to the considered net panel. The model accounts implicitly for shadow effects of twines, which matter for large net deformations. The wake velocity inside the cage without fish is considered spatially uniform and calculated according to Løland (1991)[12]. Kristiansen and Faltinsen (2012b, 2014)[13][14] conducted a series of experiments to measure the drag force on the net cage and validated their hydroelastic truss model for the net. They studied a bottomless net cage attached to both an elastic and nearly rigid floater in both current only and combined current and wave conditions. The system in current is solved as an unsteady system starting from rest in order to reach the steady condition.

The incoming flow to the fish will be influenced by the upstream part of the net cage. An illustration of the incident flow to the fish is presented in Figure 1. Furthermore, the existence of the fish will influence the incident flow to the netting. The fact that the fish will influence the incident flow to the net cage is illustrated in Figure 2.

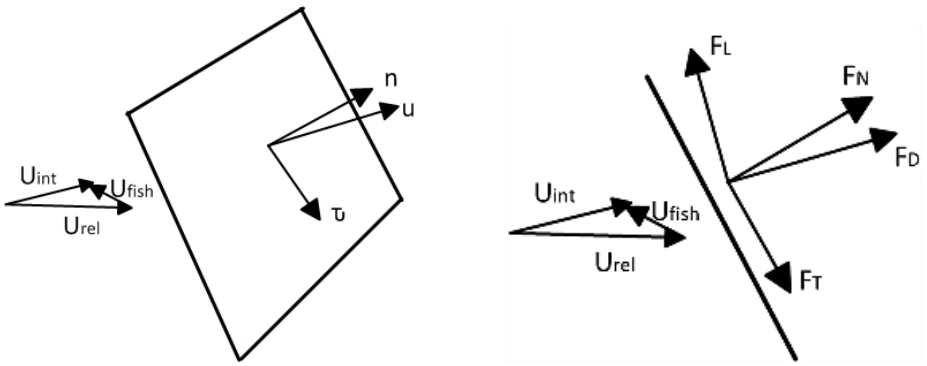

(a) Three dimensional view on the net panel

(b) Side view on the net panel

Figure 2: Inflow and forces on a net panel. (a) n is the normal unit vector of the panel, τ is the tangential unit vector of the panel, U_{rel} is the relative velocity between the incoming flow and the velocity of the net without the fish. U_{fish} is the flow velocity generated by the fish. U_{int} is the vector sum of U_{rel} and U_{fish}, and it is the incident flow to the net panel. (b) F_N is the normal component of the forces, F_T is the tangential component of the forces, F_D is the drag force acting along the incident flow U_{int}, and F_L is the lift force perpendicular to the incident flow.

3. Experiments with artificial and live fish in a net cage

Artificial fish model experiments as well as live fish experiments were performed in the Marine Cybernetics Laboratory at Norwegian University of Science and Technology (NTNU). A model test scale 1:25 is assumed in selecting current velocities and net dimensions based on Froude scaling and correct solidity ratio. The twine diameter was 0.6 mm in model scale nets, which implies that the Reynolds number with twine diameter as characteristic length is not properly scaled. If the net has the correct solidity ratio, the latter effect is secondary. Since there are in order of 100000-200000 fish in a typical fish farm cage, it is not practical to geometrically scale the fish, and only the total volume of the fish is ensured. Instead of generating current, the whole model is towed by the carriage. This ensures a uniform inflow velocity without turbulence. Most of the tests were repeated three or more times. The time interval between two tests was 10 minutes, allowing for residual currents to be reduced to an acceptably low level. Blockage effects from the tank wall and bottom in current are negligible. Wave generation by the net cage is believed small.

The bottomless net model in the artificial fish model experiments is the same as one of the models in the experiments by Kristiansen and Faltinsen (2012b, 2014)[13][14]. An inelastic circular floater supports the net and the weights. The floater is moored at the front and aft parts. The model particulars are floater diameter=1.5 m, net depth=1.3 m, cross-sectional diameter of floater=30 mm, diameter of net twines=0.6-0.8 mm, net solidity ratio $Sn = 0.32$ and mass of bottom weights in air=16×75 g. The bottom weights were made from lead. Sn was estimated by counting pixels with a photographic technique. The forward part of the longitudinal cross-section of the artificial fish with circular transverse cross-sections is a combination of a parabola and an ellipse, while a parabola describes the aft part:

$$b(x) = \begin{cases} \pm\frac{1}{2}(B\sqrt{1 - x_L^2/A^2} + B - d_1 x_L^2) & x_L < 0 \\ \pm(B - d_2 x_L^2) & x_L \geq 0 \end{cases} \tag{3}$$

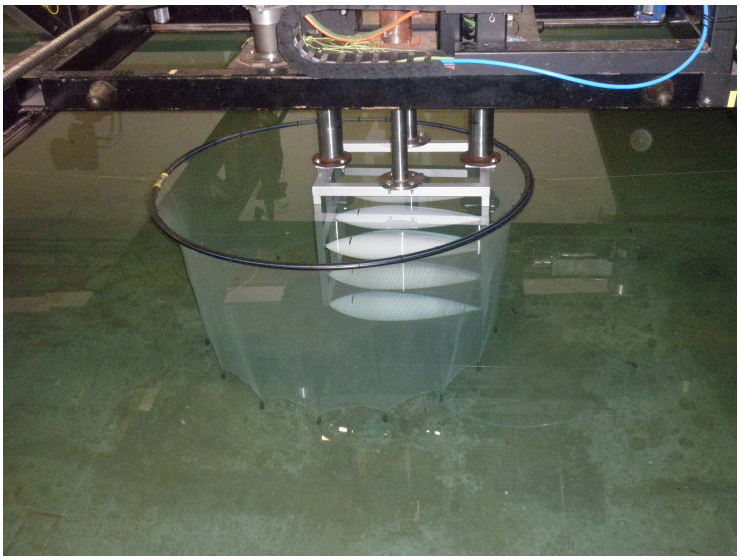

Figure 3: Photo from the experiments with nine artificial model fish arranged in a 3×3 matrix frame arrangement.

Here, $d_1 = B/A^2$, $d_2 = B/C^2$, fish length $L = 0.62\ m$, half width of the fish $B = L/8.2$, length of the front part $A = L/3$ and length of the aft part $C = 2L/3$. The fish profile and the coordinate system is shown in Figure 4.

Polyether foam plastics was used to manufacture the fish models. The surface of the fish model is painted and smoothed. We use nine equivalent fish models with the total volume of 2.5% of the volume 2.3 m^3 of the net cage at rest with an imaginary flat bottom. The nine model fish are arranged in an equidistant 3×3 matrix configuration, supported by a frame, as indicated in Figure 3. The distance between the centerlines of two neighbor fish is $3B$. One group of experiments for the net cage with frame only was conducted. The drag on the frame is then deducted from all the experimental results with artificial fish. The Reynolds numbers $Re = U_i L/\nu$ are in the range $3.1 \times 10^4 < Re < 8.7 \times 10^4$ which correspond to laminar boundary layer flows. Here $U_i = rU$ as in Figure 1, and ν is the kinematic viscosity of water.

In the live fish experiments, a closed bottom net cage was needed. A sketch of the net cage is presented in Figure 5 together with main dimensions. The

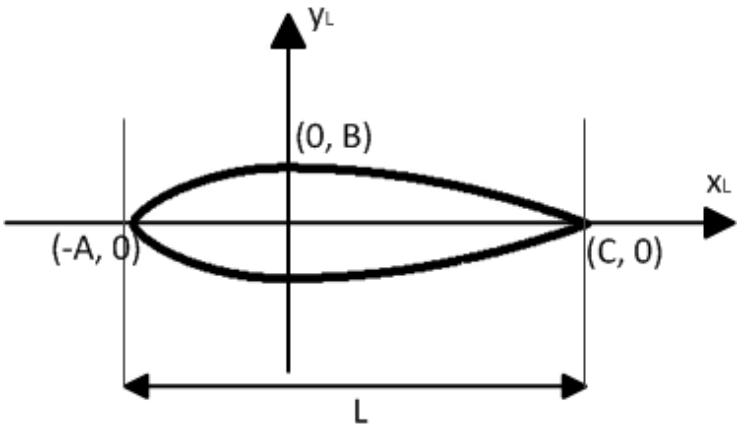

Figure 4: Fish profile. $L = 0.62\ m$, $B = L/8.2$, $A = L/3$ and $C = 2L/3$, referring to eq. (3). The coordinate system of x_L and y_L is for the definition of the fish profile.

rigid circular floater had semi-submerged circular cross-section with radius of 1.5 cm.

Additional model particulars are diameter of net twines=0.6-0.8 mm, net solidity ratio $Sn = 0.32$ and mass of bottom weights in air=$16 \times 75\ g$. SINTEF Fisheries and Aquaculture provided 928 salmons with an average length of 16 cm. The experiments were carried out according to Norwegian regulations for experiments with live animals. To make sure that the fish could stay alive during the full week of testing, a particular water environment was required. During the experiments, the temperature of the water was kept close to 11.5 $°C$ and the oxygen level in the net cage was close to 9.0 mg/L. The fish swam vigorously in the net cage until the end of the experiments which lasted for one week. The influences of two different numbers of fish were tested, i. e. 928 and 814 fish with total volume equal to 2.79% and 2.47% of the net cage volume at rest, respectively. Figure 6 is a top view photo taken in a current only experiment with 814 fish. We observed that in the current only case, most of the fish were swimming against the current except a few that made maneuvers like turning or accelerating.

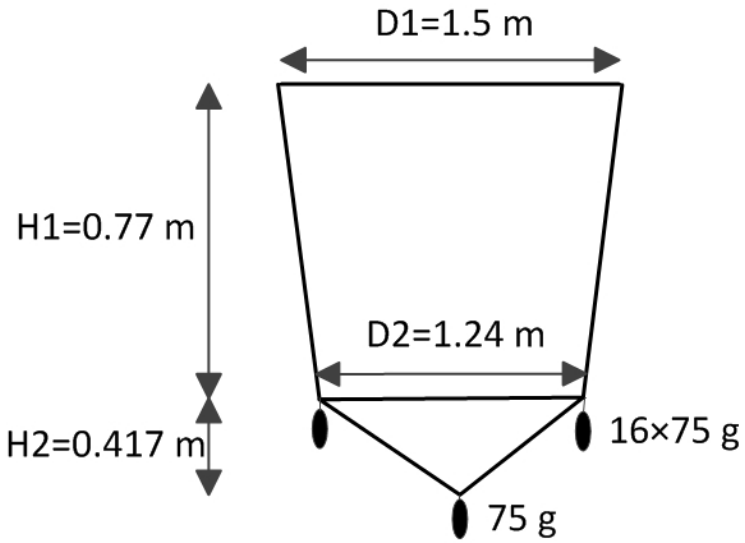

Figure 5: Sketch of the closed net cage with circular horizontal cross-sections used in the live fish experiments. The net cage was supported by a nearly rigid circular floater (not shown)

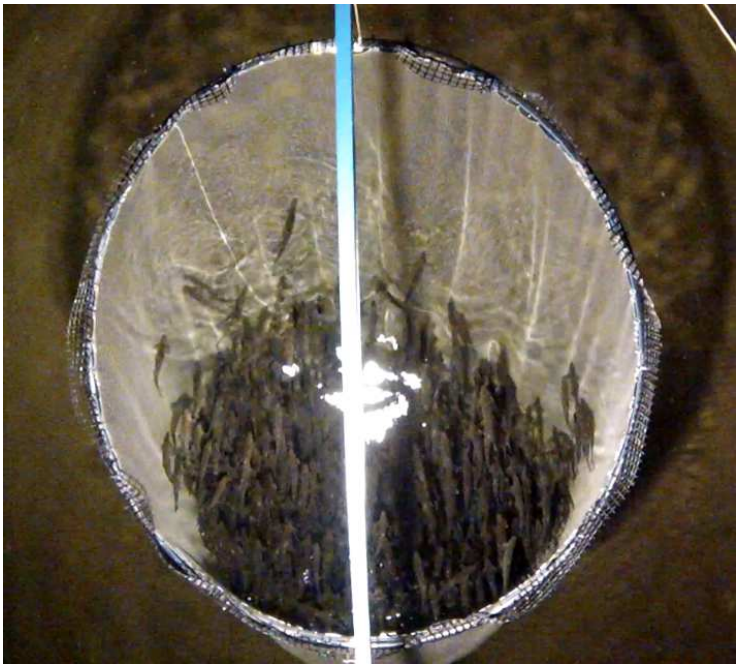

Figure 6: A top view photo of the experiment in current only for 814 fish. In this case, most of the fish were observed to swim against the current except a few that turned or accelerated.

4. Mooring loads with artificial and live fish

In this section, the content is divided into four parts: the artificial fish in current, the live fish in current, the live fish in regular waves only and the live fish in regular waves and current.

4.1. Artificial fish in current

The experimental and numerical results of the effect of the artificial fish models on the mooring loads on the net cage are first presented. In the numerical simulations, the number of transverse cross-sections on each fish body is 70 and the mesh panel on the net cage is 32×12, which means 32 trusses in horizontal and 12 trusses in vertical directions. The latter truss arrangement is artificial, but represents well the global behavior of the net (Kristiansen and Faltinsen, 2012)[11]. Because of the deformation of the net cage, the artificial fish begin to touch the front net when the towing speed is 0.14 m/s. However, in the numerical simulations, the model fish touched the front part of the cage when the current speed was equal to or higher than 0.1 m/s. When touching occurred, the numerical model broke down due to singularities associated with the source distribution representing the far-field flow of a fish. In the numerical simulations, we avoid the touching with the net by moving the fish back slowly from the front part of the net cage during simulations. By this approach, we manage to also simulate the cases when the current speeds are larger than 0.1 m/s.

The experimental and numerical drag force, F_D, and the relative drag difference $\triangle F_D/F_D$ versus current speed are presented in Figure 7 and Figure 8. Here $\triangle F_D$ is the difference in drag with and without fish. F_D is the drag without fish. The drag due to the frame is deducted, as described earlier. We note that the displacement flow effect is more significant than the wake flow effect in the numerical calculations of drag force.

Both the numerical and experimental results indicate that the mooring load influence of the artificial fish models is insignificant and is less than 3% of the no fish case. However, the quantitative agreement between theory and experiments

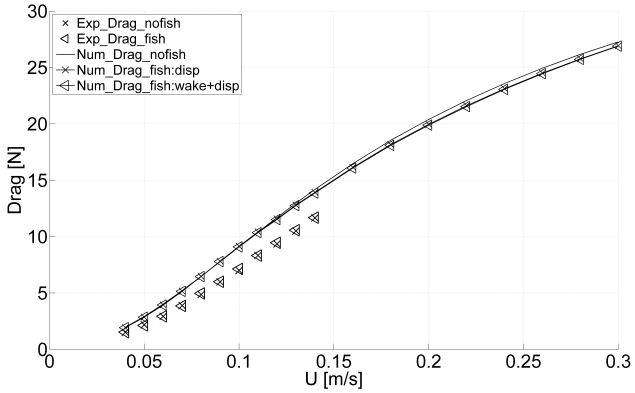

Figure 7: Experimental and numerical drag versus current speed U for the artificial fish model. Abbreviations: Num=numerical calculations. Disp=Displacement flow. Wake=Wake flow.

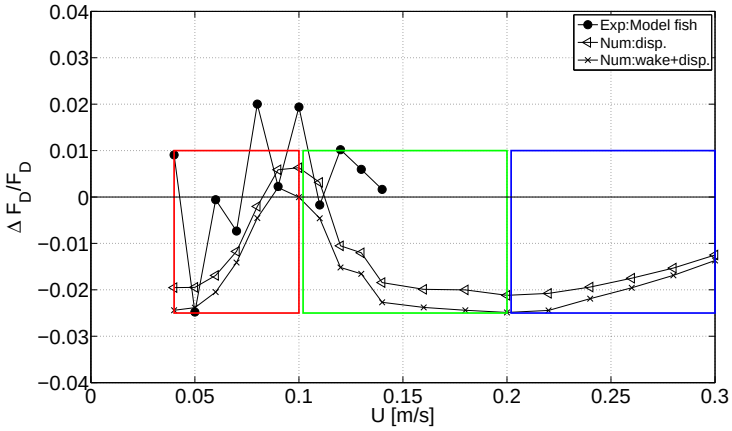

Figure 8: Experimental and numerical relative drag difference $\triangle F_D/F_D$ versus current speed U for the artificial fish model. Abbreviations: Num=numerical calculations. Disp=Displacement flow. Wake=Wake flow.

on the influence of the fish is unsatisfactory. Error sources in the numerical calculations are that the hydrodynamic interaction between the fish is neglected, that the viscous and potential flow are decoupled, the viscous wake due to a fish is empirically determined and that neither the net nor neighboring fish are in the far-fields as assumed in the theoretical model. The scatter of the experimental relative drag difference $\triangle F_D/F_D$ as a function of U could be the inaccuracy of the force measurements and the vibration of the carriage, which carries the supporting frame of the artificial fish. The decreased flow-displacement effects of the fish on the back part of the net cage due to the deformation of the net is the reason why the numerically calculated magnitude of $\triangle F_D/F_D$ as a function of U decreases with increasing U for $U < 0.11\ m/s$, as the curve in the left red box in Figure 8. The reason why the magnitude of $\triangle F_D/F_D$ increases with increasing U for $U > 0.11\ m/s$, as the curve in the middle green box in Figure 8, is that the fish are relocated closer to the back part of the net cage and the flow-displacement effects of the fish on the back part of the net cage increases. The tendency of the curve of the relative drag difference for $U > 0.2\ m/s$ to move towards zero, as the curve in the right blue box in Figure 8, is because the bottomless net cage is lifted up significantly and some of the fish come lower than the bottom edge of the net cage, which results in less influence from the fish to the net.

A numerical study was made with 514 artificial fish close to the rear part of the net and 814 artificial fish with diamond-shape distribution at different layers occupying 2.5% of the net cage volume in a rigid net cage to clarify that different distribution and numbers of fish have minor influence on our conclusions.

CFD could be attempted in order to improve the agreement between numerical and experimental results. The latter would require that net deformations are considered in the CFD calculations and require dedicated future studies.

4.2. The live fish in current

The experimental and numerical study of the live fish case in current is presented in this section. Figure 9 presents experimental drag force versus

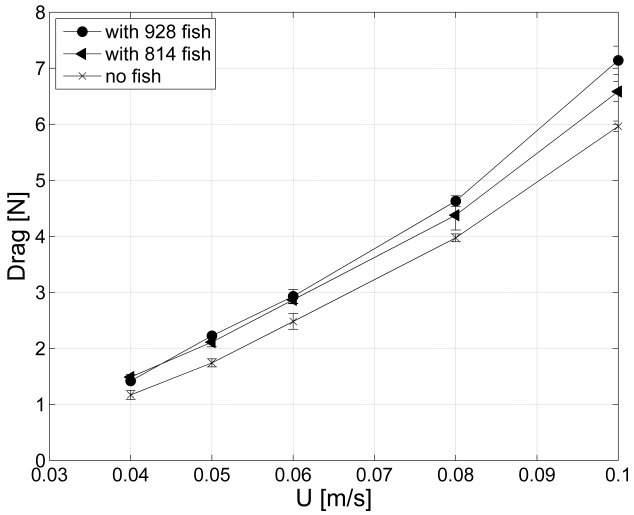

Figure 9: Drag force (mooring load) on the net cage versus current speed in live fish experiments without waves. The solid line with circles represents the mean values for the case with 928 fish, the solid line with triangles represents mean values for the case with 814 fish and the solid line with x represents the mean drag without fish.

current speed without fish and with 814 and 928 live fish for towing velocities up to 0.1 m/s. The tank length prohibited higher speeds. The standard deviation without fish obtained from repetition tests is about 1% and for the case with fish the standard deviation are all less than 5%, except the case with 814 fish when U is 0.08 m/s for which the standard deviation is 6%. All the standard deviations are at the 95% confidence level. Figure 11 presents the corresponding values of the relative difference $\triangle F_D/F_D$ of drag force with and without fish.

The drag force on the net cage due to the live fish is between 10% and 28% higher than that for the empty net cage. This applies to both fish cases, and for the whole towing velocity range. Even though the relative drag difference decreases with the current speed, the drag difference increase with the current speed as illustrated in Figure 10. In the artificial fish case, the fish caused a difference of only about 3%. It was observed during the tests with current only that the fish gathered in the lower rear part of the net cage, and significant

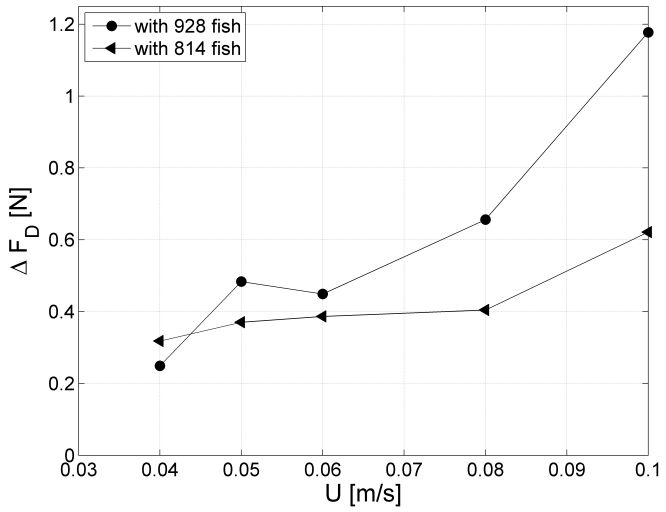

Figure 10: The difference in drag force versus current speed in live fish experiments without waves. $\triangle F_D$ is the drag difference between the cases with fish and without fish.

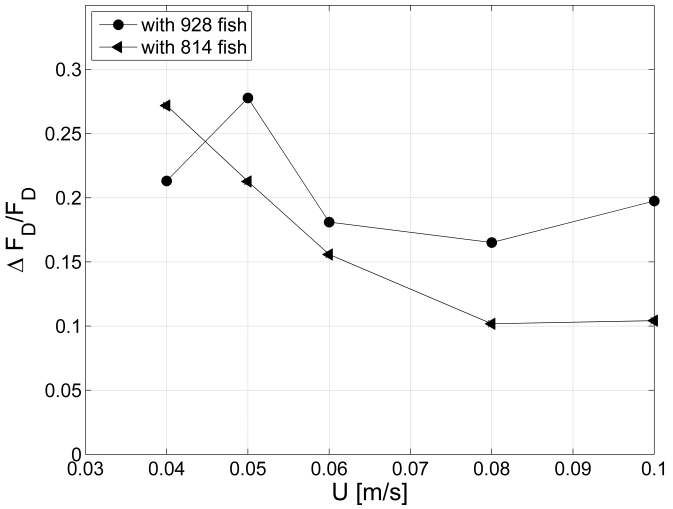

Figure 11: The relative difference of the drag force versus current speed in live fish experiments without waves. $\triangle F_D$ is the drag difference between the cases with fish and without fish. F_D is the drag force without fish.

Figure 12: Side view photo from the live fish experiment with $U = 0.10\ m/s$. The area encircled indicates the observed touching area between the fish and the net

touching of the net occurred. A picture that clearly shows the touching between the fish and the net is presented in Figure 12.

The difference in the drag of the net between 928 fish and 814 fish case is believed to be mainly due to the different numbers of the fish touching the net which tends to block the flow at the touching area of the net.

The touching area is encircled in Figure 13 for the case with 814 fish in current only. In practice, the touching leads to a higher solidity ratio at this portion of the net. We used 84% of the rear half of the cone part and 18% of the rear half of the cylinder part of the net as the touching area. A locally high solidity ratio was applied for this part of the net in the numerical simulations. The procedure was to gradually increase the local solidity ratio until the calculated and experimental net shapes were similar. The resulting calculated net shapes and calculated local additional solidity ratios are presented in Figure 13 for different towing speeds. Even though the increased local Sn, which affects the local drag coefficient C_D on the net, is lower for $U = 0.08\ m/s$ and $U = 0.10\ m/s$ than for $U < 0.08\ m/s$, the drag difference is increased because it is proportional to C_D and U^2. Furthermore, the lift force is influenced by the increased local Sn,

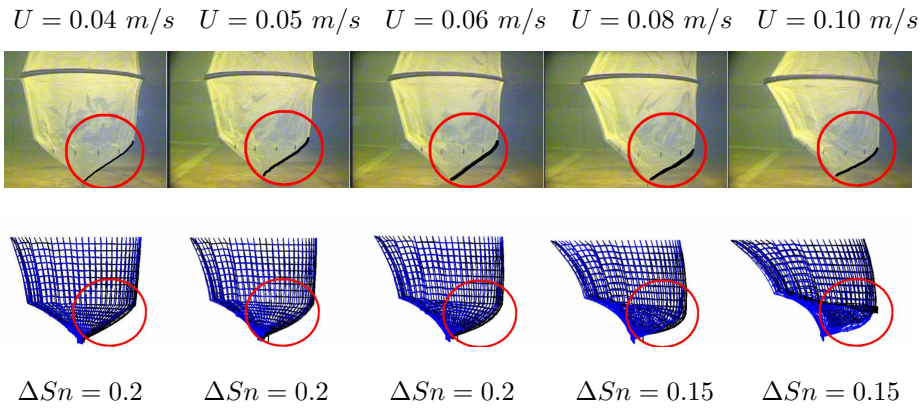

Figure 13: Net deformation in the experiment with 814 live fish (upper row) and the numerical simulations (lower row) for current velocities between 0.04 m/s and 0.10 m/s. The area inside the red circle indicates the touching area. We used 84% of the rear half of the cone part and 18% of the rear half of the cylinder part of the net as the touching area. The black area highlighted in the red circle is the deformed part. ΔSn represents the increased solidity ratio at the back cone part of the cage used in the calculations.

which means that the local deformation of the net is influenced as well.

The relative difference in drag between the numerical calculations and the drag force from the experiments without fish are presented in Figure 14 together with a sensitivity study of the applied ΔSn in Figure 13 in the range of ± 0.04 with an increment of 0.01. Comparisons are made with the experimental relative drag differences in the case with 814 fish earlier presented in Figure 11. Since the agreement between numerical and experimental values is satisfactory both when it comes to net deformation and drag force, we believe that the touching between the fish and the net is the cause of the non-negligible increased drag on the net cage.

4.3. Live fish in regular waves

When we ran the experiment in regular waves only, the fish was observed to swim with an individual behaviour rather than a stationary group behaviour as in current only. Furthermore, some of the fish went to the bottom of the net possibly due to that the fish was uncomfortable in the wave zone leading to that the fish already occupying the bottom was squeezed towards the bottom net and

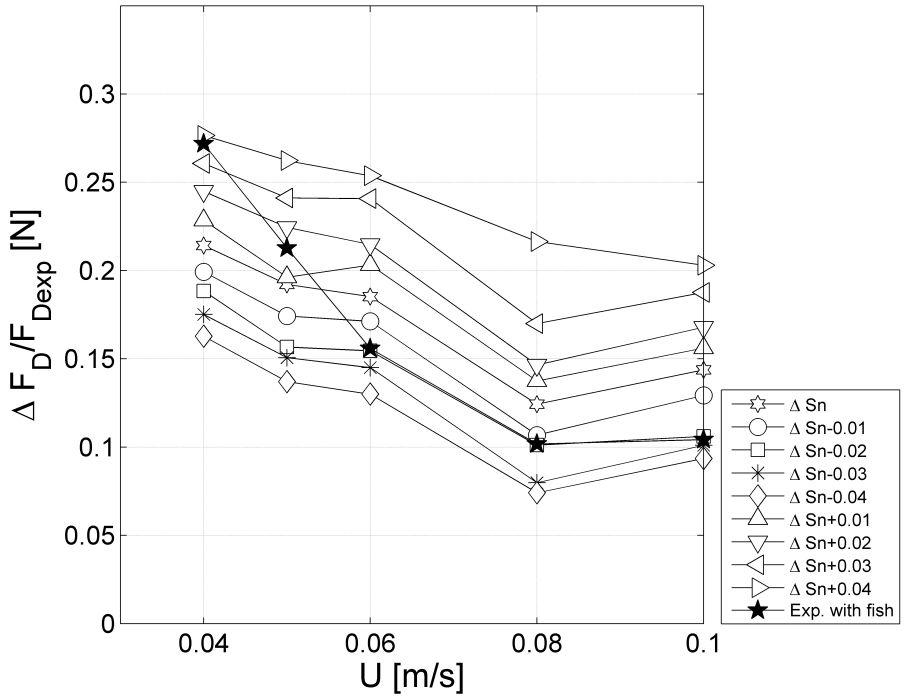

Figure 14: Comparison between the relative drag difference in the numerical simulations and the experiment with 814 live fish versus current speed. F_{Dexp} = experimental drag without fish. ΔSn represent the value in Figure 13, $\Delta Sn - 0.01$ represent the value in Figure 13 minus 0.01, etc. For instance, when $U = 0.04\ m/s$, $0.05\ m/s$, $0.06\ m/s$, $0.08\ m/s$ and $0.10\ m/s$, ΔSn represents 0.2, 0.2, 0.2, 0.15 and 0.15 separately and $\Delta Sn - 0.01$ represents 0.19, 0.19, 0.19, 0.14 and 0.14 separately. The same for the other symbols

touching the net. The fish swimming behaviour in waves would influence the incident flow to the net and the fish in the bottom appeared to have effectively acted as a bottom weight, which influenced the net shape and thereby the mooring loads. The bottom weight effect depends on the change of buoyancy of the fish due to the increase and decrease of the volume of the swim bladder. We are unable to numerically quantify the effects. One reason is that the volumes of the swim bladders of the fish are unknown. Thus the results are based on our observations and measurements. The experimental wave periods were 1.0 s, 1.2 s and 1.4 s with wave steepnesses H/λ=1/45, 1/30 and 1/15. Here H is the wave height and λ is the wavelength. A steady time interval was used to calculate the significant mooring load amplitude $F_a = \sqrt{2}\sigma_F$. Here σ_F means the standard deviation in the considered time interval. The relative influence of fish on the mooring load amplitude was -6.2%, 16.6% and 6.3% for wave periods 1.0 s, 1.2 s and 1.4 s, respectively.

4.4. Live fish in combined regular wave and current

We also conducted experiments with combined regular waves and current. The wave propagation direction was opposite to the towing carriage direction. Three cases with combined regular waves and current were considered. A wave period of 1.2 s and a wave steepness of $H/\lambda = 1/30$ were used in all cases. The current velocities were $U = 0.04\ m/s$, $0.05\ m/s$ and $0.06\ m/s$. When the current was added to the waves, there was less touching between the fish and aft part of the net of the type that occurred in current only. A factor may be the wave induced oscillations of the net. Furthermore, less bottom touching than in the wave only case was observed because the fish were more active to move against the current instead of going down to the bottom.

Similarly as in the wave only cases, a steady time interval is used to calculate the mean drag and the significant drag amplitude. The maximum force is estimated as the sum of the mean force and the significant force amplitude. Strictly speaking this is only true for purely harmonic signals. The mean and maximum drag with and without fish are presented in Figure 15. Both absolute

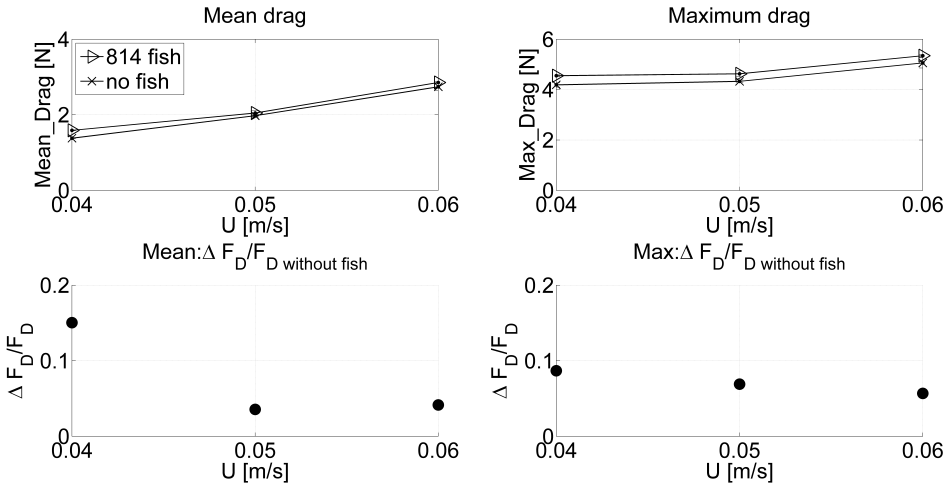

Figure 15: Experimental mean and maximum drag force for three current speeds in combined wave and current with wave period 1.2 s and wave steepness 1/30. $\triangle F_D$ represents difference in the mean or maximum drag between the cases with and without fish. $F_{D\ without\ fish}$ represents the mean or maximum drag force without fish.

values and relative differences are plotted in the figure. The standard deviation from repetition tests is less than 3% with a 95% confidence level. As the results in Figure 15 show, the relative difference of the mean and maximum value of the drag force is lower than 10% of the no fish case except for the mean value in the case with current speed 0.04 m/s. The relative difference is then 15%.

5. Concluding remarks

This paper describes a numerical and experimental study of the influence of a fish group on the mooring loads of a net cage with circular rigid floater in ambient current and waves.

Both artificial and live fish setups are considered. In the artificial fish experiments in current, a bottomless net cage was employed and nine equivalent rigid fish models in a 3×3 matrix arrangement with total volume of 2.5% of the fish cage at rest were used to represent the displaced volume of all fish in a real

fish farm cage. The results from the experiments indicated that the influence of the nine artificial fish models on the mooring load was less than 3%.

In the live fish experiments, more than 800 salmons of a length 16 cm occupied a closed bottom net cage. The mooring loads with fish in current were between 10% and 28% larger than the loads without fish. The reason is contact mainly between the fish and the back cone part of the net cage.

Numerical simulations of the interaction between the fish and the net cage were conducted in current. A potential-flow slender-body theory was applied in the artificial-fish case to calculate the displacement flow caused by the fish. An empirical viscous wake flow was added. The displacement flow was clearly more important than the wake flow. The numerical mooring loads were qualitatively in agreement with the experiments. The numerical procedure in the live fish case were different and based on experimental observations of the contact between the fish and net. The solidity ratio in the contact area was increased so that the experimental and numerical net deformations agree. Although somewhat smaller, the same order of difference for the mooring loads as seen in the live fish experiment was obtained from our simulations.

The experiments in waves and combined waves and current also showed a non-negligible influence of the fish on the mooring loads. The waves caused the fish to swim in an individual behaviour rather than a stationary group behaviour as in current only. Some of the fish went to the bottom of the net possibly due to that the fish was uncomfortable in the wave zone. The fish swimming behaviour in waves would influence the incident flow to the net and the fish in the bottom appeared to have effectively acted as a bottom weight, which influenced the net shape and thereby the mooring loads. We are unable to numerically quantify that effect. One reason is that the volumes of the swim bladders of the fish are unknown.

Since our numerical model depends on experimental observations, we need to develop rational procedures for how many fish touch the net in current and how the fish behave and how many of them go to the bottom of the net in waves. An unanswered question is if the fish behavior in full scale is the same

as in model scale.

If the fish farm is equipped with supporting vertical chains or ropes, the local net deformation due to fish contact may cause contact between the net and the chains/ropes. The consequence can be net rupture with resulting fish escape. Further studies are needed.

Acknowledgments

The Research Council of Norway through the Centres of Excellence funding scheme AMOS, project number 223254 and Centre for research-based innovations funding CREATE, project number 174842, supported this work.

References

[1] Ø. Jensen, T. Dempster, E. B. Thorstad, I. Uglem, A. Fredheim, Escapes of fishes from norwegian sea-cage aquaculture: causes, consequences and prevention, Aquaculture Environment Interactions 1 (1) (2010) 71–83.

[2] A. Chacon-Torres, L. Ross, M. Beveridge, The effects of fish behaviour on dye dispersion and water exchange in small net cages, Aquaculture 73 (1-4) (1988) 283–293.

[3] D. Johansson, F. Laursen, A. Fernö, J. E. Fosseidengen, P. Klebert, L. H. Stien, T. Vågseth, F. Oppedal, The interaction between water currents and salmon swimming behaviour in sea cages, PloS one 9 (5) (2014) e97635.

[4] H. W. Rasmussen, Ø. Patursson, K. Simonsen, Visualisation of the wake behind fish farming sea cages, Aquacultural Engineering 64 (2015) 25–31.

[5] H. Winthereig-Rasmussen, K. Simonsen, Ø. Patursson, Flow through fish farming sea cages: Comparing computational fluid dynamics simulations with scaled and full-scale experimental data, Ocean Engineering 124 (2016) 21–31.

[6] J. Newman, T. Wu, A generalized slender-body theory for fish-like forms, Journal of Fluid Mechanics 57 (04) (1973) 673–693.

[7] M. Wolfgang, J. Anderson, M. Grosenbaugh, D. Yue, M. Triantafyllou, Near-body flow dynamics in swimming fish, Journal of Experimental Biology 202 (17) (1999) 2303–2327.

[8] R. D. Blevins, Applied fluid dynamics handbook, New York, Van Nostrand Reinhold Co., 1984, 568 p. 1.

[9] J. N. Newman, Marine hydrodynamics, MIT press, 1977.

[10] R. Skejic, O. M. Faltinsen, A unified seakeeping and maneuvering analysis of ships in regular waves, Journal of marine science and technology 13 (4) (2008) 371–394.

[11] T. Kristiansen, O. M. Faltinsen, Modelling of current loads on aquaculture net cages, Journal of Fluids and Structures 34 (2012) 218–235.

[12] G. Løland, Current forces on and flow through fish farms, Division of Marine Hydrodynamics, the Norwegian Institute of Technology, 1991.

[13] T. Kristiansen, O. Faltinsen, Mooring loads of a circular net cage with an elastic floater in waves and current, in: 6th Int. Conf. on Hydroelasticity in Marine Technology, 2012.

[14] T. Kristiansen, O. M. Faltinsen, Experimental and numerical study of an aquaculture net cage with floater in waves and current, Journal of Fluids and Structures 54 (2015) 1–26.